PHYSICAL REVIEW D **92,** 031101(R) (2015)

# Spectroscopy of geoneutrinos from 2056 days of Borexino data

M. Agostini,[1] S. Appel,[1] G. Bellini,[2] J. Benziger,[3] D. Bick,[4] G. Bonfini,[5] D. Bravo,[6] B. Caccianiga,[2] F. Calaprice,[7] A. Caminata,[8] P. Cavalcante,[5] A. Chepurnov,[9] K. Choi,[10] D. D'Angelo,[2] S. Davini,[11] A. Derbin,[12] L. Di Noto,[8] I. Drachnev,[11] A. Empl,[13] A. Etenko,[14] G. Fiorentini,[15] K. Fomenko,[16] D. Franco,[17] F. Gabriele,[5] C. Galbiati,[7] C. Ghiano,[8] M. Giammarchi,[2] M. Goeger-Neff,[1] A. Goretti,[7] M. Gromov,[9] C. Hagner,[4] T. Houdy,[18] E. Hungerford,[13] Aldo Ianni,[5] Andrea Ianni,[7] K. Jedrzejczak,[19] M. Kaiser,[4] V. Kobychev,[20] D. Korablev,[16] G. Korga,[5] D. Kryn,[17] M. Laubenstein,[5] B. Lehnert,[21] E. Litvinovich,[14,22] F. Lombardi,[5] P. Lombardi,[2] L. Ludhova,[2] G. Lukyanchenko,[14,22] I. Machulin,[14,22] S. Manecki,[6] W. Maneschg,[23] F. Mantovani,[15] S. Marcocci,[11] E. Meroni,[2] M. Meyer,[4] L. Miramonti,[2] M. Misiaszek,[19,5] M. Montuschi,[15] P. Mosteiro,[7] V. Muratova,[12] B. Neumair,[1] L. Oberauer,[1] M. Obolensky,[17] F. Ortica,[24] K. Otis,[25] L. Pagani,[8] M. Pallavicini,[8] L. Papp,[1] L. Perasso,[8] A. Pocar,[25] G. Ranucci,[2] A. Razeto,[5] A. Re,[2] B. Ricci,[15] A. Romani,[24] R. Roncin,[5,17] N. Rossi,[5] S. Schönert,[1] D. Semenov,[12] H. Simgen,[23] M. Skorokhvatov,[14,22] O. Smirnov,[16] A. Sotnikov,[16] S. Sukhotin,[14] Y. Suvorov,[26,14] R. Tartaglia,[5] G. Testera,[8] J. Thurn,[21] M. Toropova,[14] E. Unzhakov,[12] R. B. Vogelaar,[6] F. von Feilitzsch,[1] H. Wang,[26] S. Weinz,[27] J. Winter,[27] M. Wojcik,[19] M. Wurm,[27] Z. Yokley,[6] O. Zaimidoroga,[16] S. Zavatarelli,[8] K. Zuber,[21] and G. Zuzel[19]

(Borexino Collaboration)

[1]*Physik-Department and Excellence Cluster Universe, Technische Universität München, 85748 Garching, Germany*
[2]*Dipartimento di Fisica, Università degli Studi e INFN, 20133 Milano, Italy*
[3]*Chemical Engineering Department, Princeton University, Princeton, New Jersey 08544, USA*
[4]*Institut für Experimentalphysik, Universität, 22761 Hamburg, Germany*
[5]*INFN Laboratori Nazionali del Gran Sasso, 67010 Assergi (AQ), Italy*
[6]*Physics Department, Virginia Polytechnic Institute and State University, Blacksburg, Virginia 24061, USA*
[7]*Physics Department, Princeton University, Princeton, New Jersey 08544, USA*
[8]*Dipartimento di Fisica, Università degli Studi e INFN, Genova 16146, Italy*
[9]*Lomonosov Moscow State University Skobeltsyn Institute of Nuclear Physics, 119234 Moscow, Russia*
[10]*Department of Physics and Astronomy, University of Hawaii, Honolulu, Hawaii 96822, USA*
[11]*Gran Sasso Science Institute (INFN), 67100 Ł'Aquila, Italy*
[12]*St. Petersburg Nuclear Physics Institute NRC Kurchatov Institute, 188350 Gatchina, Russia*
[13]*Department of Physics, University of Houston, Houston, Texas 77204, USA*
[14]*NRC Kurchatov Institute, 123182 Moscow, Russia*
[15]*Dipartimento di Fisica e Scienze della Terra Università degli Studi di Ferrara e INFN, Via Saragat 1-44122, Ferrara, Italy*
[16]*Joint Institute for Nuclear Research, 141980 Dubna, Russia*
[17]*AstroParticule et Cosmologie, Université Paris Diderot, CNRS/IN2P3, CEA/IRFU, Observatoire de Paris, Sorbonne Paris Cité, 75205 Paris Cedex 13, France*
[18]*Commissariat a l'Energie Atomique et aux Energies Alternatives, Centre de Saclay, IRFU, 91191 Gif-sur-Yvette, France*
[19]*M. Smoluchowski Institute of Physics, Jagiellonian University, 30059 Krakow, Poland*
[20]*Kiev Institute for Nuclear Research, 06380 Kiev, Ukraine*
[21]*Department of Physics, Technische Universität Dresden, 01062 Dresden, Germany*
[22]*National Research Nuclear University MEPhI (Moscow Engineering Physics Institute), 115409 Moscow, Russia*
[23]*Max-Planck-Institut für Kernphysik, 69117 Heidelberg, Germany*
[24]*Dipartimento di Chimica, Biologia e Biotecnologie, Università e INFN, 06123 Perugia, Italy*
[25]*Amherst Center for Fundamental Interactions and Physics Department, University of Massachusetts, Amherst, Massachusetts 01003, USA*
[26]*Physics and Astronomy Department, University of California Los Angeles (UCLA), Los Angeles, California 90095, USA*
[27]*Institute of Physics and Excellence Cluster PRISMA, Johannes Gutenberg-Universität Mainz, 55099 Mainz, Germany*

(Received 25 June 2015; published 7 August 2015)

We report an improved geoneutrino measurement with Borexino from 2056 days of data taking. The present exposure is $(5.5 \pm 0.3) \times 10^{31}$ proton × yr. Assuming a chondritic Th/U mass ratio of 3.9, we obtain $23.7^{+6.5}_{-5.7}(\text{stat})^{+0.9}_{-0.6}(\text{sys})$ geoneutrino events. The null observation of geoneutrinos with Borexino alone has a probability of $3.6 \times 10^{-9}$ ($5.9\sigma$). A geoneutrino signal from the mantle is obtained at 98% C.L.

 

The radiogenic heat production for U and Th from the present best-fit result is restricted to the range 23–36 TW, taking into account the uncertainty on the distribution of heat producing elements inside the Earth.

DOI: 10.1103/PhysRevD.92.031101 PACS numbers: 13.15.+g, 29.40.Mc, 91.35.-x, 91.67.Qr

Geoneutrinos are electron antineutrinos ($\bar{\nu}_e$) produced by $\beta$ decays of long-lived isotopes, which are naturally present in the interior of the Earth, such as decays in the $^{238}$U and $^{232}$Th chains, and $^{40}$K [1,2]. Geo-$\bar{\nu}_e$ measurements have been reported by Borexino [3,4] and KamLAND [5,6]. Here we present improved reactor neutrino and geo-$\bar{\nu}_e$ measurements performed by Borexino. Borexino is an unsegmented liquid scintillator detector in operation at the underground Gran Sasso National Laboratory, Italy [7]. In liquid scintillator detectors $\bar{\nu}_e$ are detected via the inverse $\beta$ decay process, $\bar{\nu}_e + p \rightarrow e^+ + n$, with a threshold of 1.806 MeV. The deposited $\bar{\nu}_e$ energy results in a prompt signal induced by the positron, and includes annihilation photons. The visible energy is related to the $\bar{\nu}_e$ energy as $E_{\rm vis} = E_{\bar{\nu}_e} - 0.784$ MeV. A delayed signal induced by the neutron capture on protons produces the 2.22 MeV gamma-ray, providing a delayed coincidence signal with a mean capture time of $259.7 \pm 1.3(\text{stat}) \pm 2.0(\text{syst})$ $\mu$s [8]. In Borexino 278 tons of ultrapure organic liquid scintillator (pseudocumene doped with 1.5 g/l of diphenyloxazole) is confined within a thin, spherical nylon inner vessel (IV) with a nominal radius of 4.25 m and concentrically placed inside a stainless steel sphere (SSS) with radius of 13.7 m and equipped with 2212 8" photomultipliers (PMTs). The volume between the SSS and the IV, divided in two regions by a second outer nylon vessel (OV) is filled with 890 tons of pseudocumene with 3 g/l of light quencher dimethylphthalate to shield the core of the detector against $\gamma$ radiation and radon from the PMTs and the SSS. The SSS is immersed in a water tank (WT) instrumented with 208 PMTs as a Čerenkov active muon veto, also acting as an shield against $\gamma$-rays and neutrons from the surrounding rock.

In Borexino, known sources of $\bar{\nu}_e$ events are nuclear reactors and geoneutrinos. For geoneutrinos, $^{238}$U and $^{232}$Th are the only isotopes abundant enough to significantly contribute events in Borexino above the inverse $\beta$ decay threshold. The light yield in Borexino is measured to be about 500 photoelectrons (p.e.) / MeV and the energy resolution scales as $\sim 5\%/\sqrt{(E)}$ [7]. The Borexino liquid scintillator shows a high pulse shape discrimination efficiency in separating high ionizing particles (protons, $\alpha$'s) from electrons and gamma-rays [9].

The data reported here were collected between December 15, 2007 and March 8, 2015 for a total of 2055.9 days before any selection cut. The number of PMTs for the present data set has been declining with time, from 1931 to 1525 (average 1730), with small run by run fluctuations. As reported in [3] the event energy is a calibrated nonlinear function of the number of detected p.e. We perform the analysis directly in number of p.e. We discard events occurring within 2 ms of every muon crossing the outer detector and within 2 s of muons crossing the inner detector to reject neutrons and long-lived cosmogenic radioactivity, respectively. This cut reduces the live-time to 1841.9 days. We apply the following additional selection cuts: (1) prompt scintillation light: $Q_p > 408$ p.e. (i.e., 1.022 MeV corrected for the energy resolution); (2) delayed signal scintillation light: $860 < Q_d < 1300$ p.e. (neutron capture peak); (3) correlation distance between prompt and delayed signals: $\Delta R < 1$ m; (4) correlated time between prompt and delayed signals: $20 < \Delta t < 1280$ $\mu$s; (5) pulse shape discrimination with Gatti filter [10]: $g_{\alpha\beta} < 0.015$ for delayed signals; (6) multiplicity cut: selected event are neither preceded or followed by neutron-like events within a 2 ms window; (7) dynamical fiducial volume [9]: every prompt signal has a reconstructed vertex $> 30$ cm away from the time-varying IV surface; (8) FADC cut: independent check of candidate events features by a 400 MHz digitizer acquisition system. The combined efficiency of the cuts is determined by Monte Carlo to be $(84.2 \pm 1.5)\%$. The total efficiency-corrected exposure for the present data set is $907 \pm 44$ ton $\times$ yr. We have identified 77 $\bar{\nu}_e$ candidates passing all the selection cuts.

The probability of $\bar{\nu}_e$-mimicking background events leaking into the data set was evaluated as follows: (i) The rate of accidental coincidences has been searched for by shifting the delayed time window to 2–20 seconds and keeping all other cuts unchanged. The energy spectrum of these events is limited to $< 3$ MeV. (ii) Time correlated events have been searched for in the (2 ms, 2 s) time window. A negligible amount of correlated events with a $\sim$1 s time constant were identified and their contribution in the $\bar{\nu}_e$ time window determined. (iii) $(\alpha, n)$ background for $\bar{\nu}_e$ search has been extensively discussed elsewhere [3–6,11]. The average rate of $^{210}$Po in the data set is determined to be $(14.1 \pm 0.2)$ counts/(day $\cdot$ ton). (iv) Cosmogenic radioactive isotopes which decay via $\beta + \text{n}$, namely $^9$Li-$^8$He [8], have been studied in the (2 ms, 2 s) time window after a muon crossing the inner detector. These events have a wide energy spectrum with maximum at $\sim$5 MeV. (5) $^{222}$Run in the liquid scintillator can produce background events through time-correlated $\beta + (\alpha + \gamma)$ decays of $^{214}$Bi and $^{214}$Po. This decay sequence has a time constant close to the neutron capture time following a $\bar{\nu}_e$ interaction. This background has been estimated by individually tagging $^{214}$Bi-$^{214}$Po decays. (vi) Backgrounds from fast neutrons, untagged muons

TABLE I. Estimated backgrounds for $\bar{\nu}_e$ given in number of events. Upper limits are given for 90% C.L.

| | |
|---|---|
| $^9$Li-$^8$He | $0.194^{+0.125}_{-0.089}$ |
| Accidental coincidences | $0.221 \pm 0.004$ |
| Time correlated | $0.035^{+0.029}_{-0.028}$ |
| $(\alpha, n)$ in scintillator | $0.165 \pm 0.010$ |
| $(\alpha, n)$ in buffer | <0.51 |
| Fast n's ($\mu$ in WT) | <0.01 |
| Fast n's ($\mu$ in rock) | <0.43 |
| Untagged muons | $0.12 \pm 0.01$ |
| Fission in PMTs | $0.032 \pm 0.003$ |
| $^{214}$Bi-$^{214}$Po | $0.009 \pm 0.013$ |
| Total | $0.78^{+0.13}_{-0.10}$ |
| | <0.65(combined) |

and spontaneous fission decays in the PMTs are the same as in previous papers [3,4]. Table I summarizes the estimated backgrounds for $\bar{\nu}_e$ candidates, expressed in number of events. The combined upper limit is obtained by Monte Carlo. The $\bar{\nu}_e$ signal-to-background ratio is ~100.

We have performed an unbinned likelihood fit of the energy spectrum of selected prompt $\bar{\nu}_e$ candidate events [3], shown in Fig. 1. The reactor and geoneutrinos spectra are obtained by Monte Carlo and the backgrounds considered in this analysis are reported in Table I. The Monte Carlo spectra have been determined as reported in [4]. The reactor neutrinos signal has been calculated adopting the data from IAEA [12] updated to 2014 and the method described in [13]. For the first quarter of 2015 we have used the values from 2014. For the present exposure we predict $(87 \pm 4)$ TNU events from nuclear reactors, where 1 Terrestrial Neutrino Unit $(\mathrm{TNU}) = 1$ event/year/$10^{32}$ protons. The log-likelihood function has two signal components, $S_{\mathrm{geo}}$ and $S_{\mathrm{react}}$, left free, and three background components, $S_{\mathrm{LiHe}}$, $S_{\alpha n}$, $S_{\mathrm{acc}}$, constrained to the values and errors reported in Table I. These components account for 75% of the total background. The other components were left out due to the uncertainty in their energy spectrum. Combined, they contribute ~1% to the best fit and their contribution to the systematic uncertainty is absorbed in the uncertainty on the energy scale.

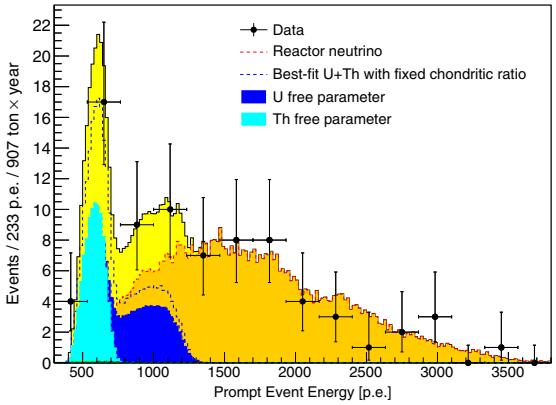


FIG. 1 (color online). Prompt light yield spectrum, in units of photoelectrons (p.e.), of anti-neutrino candidates and best-fit. The best-fit shows the total contribution of geoneutrino, reactor neutrino and background (yellow colored area) and reactor neutrino (orange colored area) assuming the chondritic ratio. The result of a separate fit with U (blue colored area) and Th (light-blue colored area) set as free and independent parameters is also shown.

Using the value ratio for the masses of Th and U, $m(\mathrm{Th})/m(\mathrm{U}) = 3.9$, suggested by the chondritic model, our best fit yields $S_{\mathrm{geo}} = 23.7^{+6.5}_{-5.7}(\mathrm{stat})^{+0.9}_{-0.6}(\mathrm{sys})$ events $[43.5^{+11.8}_{-10.4}(\mathrm{stat})^{+2.7}_{-2.4}(\mathrm{sys})$ TNU] and $S_{\mathrm{react}} = 52.7^{+8.5}_{-7.7}(\mathrm{stat})^{+0.7}_{-0.9}(\mathrm{sys})$ events $[96.6^{+15.6}_{-14.2}(\mathrm{stat})^{+4.9}_{-5.0}(\mathrm{sys})$ TNU]. When expressing the results in TNU, systematic uncertainties from both the exposure (4.8%) and the Monte Carlo energy calibration (1%) are included. Only the Monte Carlo calibration uncertainty is relevant when using the number of decays.

In Fig. 2 we show the 1, 3 and 5$\sigma$ contours from the log-likelihood fit. Borexino alone observes geoneutrinos with 5.9$\sigma$ significance (Fig. 2). The null hypothesis for geoneutrino observation has a probability equal to $3.6 \times 10^{-9}$. The measured geoneutrino signal corresponds to $\bar{\nu}_e$ fluxes at the detector from decays in the U and Th chains of $\phi(\mathrm{U}) = (2.7 \pm 0.7) \times 10^6\,\mathrm{cm}^{-2}\,\mathrm{s}^{-1}$ and $\phi(\mathrm{Th}) = (2.3 \pm 0.6) \times 10^6\ \mathrm{cm}^{-2}\,\mathrm{s}^{-1}$, respectively. Statistical and systematic uncertainties are added in quadrature.

Figure 3 shows the probability contours obtained by performing the fit leaving the U and Th spectral contributions as free parameters. The U and Th best-fit contributions are shown in Fig. 1. This measurement shows how Borexino, with larger exposure, could separate the contributions from U and Th, and demonstrates the ability of this detection technique to perform real-time spectroscopy of geoneutrinos.

The radiogenic heat production for U and Th, H(U + Th), from the present best-fit result is restricted

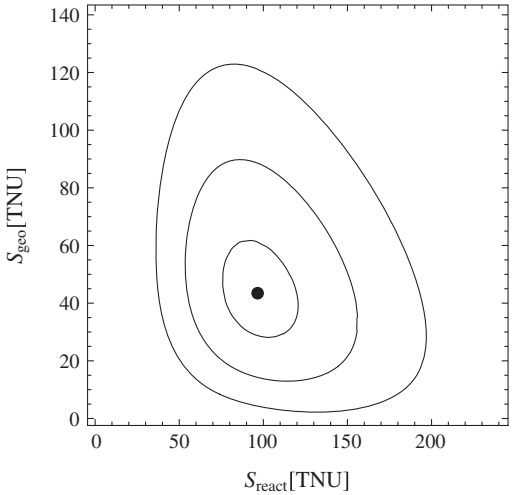


FIG. 2. Best-fit contours for 1, 3 and 5$\sigma$ for the statistics reported in this paper.

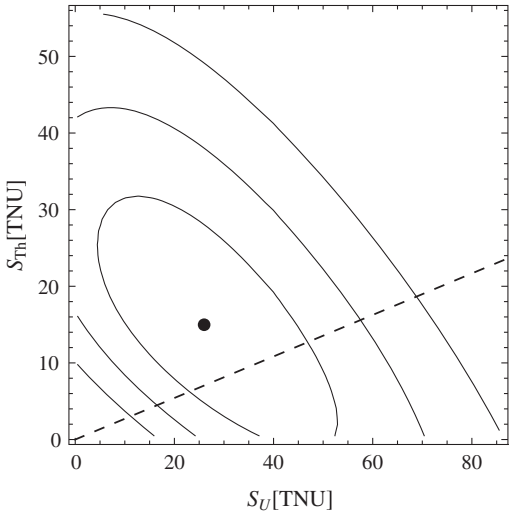


FIG. 3. Best-fit contours for 1, 2 and $3\sigma$ for the statistics reported in this paper and for an unbinned likelihood fit with U and Th kept as distinct and free parameters. All other parameters in the fit were kept unchanged. Dashed line corresponds to the chondritic assumption.

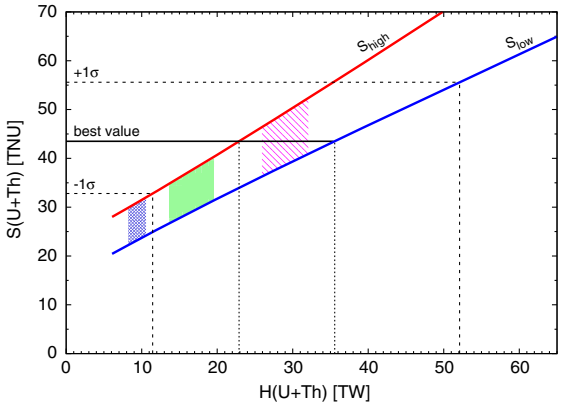


FIG. 4 (color online). The expected geoneutrino signal in Borexino from U and Th as a function of radiogenic heat released in radioactive decays of U and Th [2]. The three filled regions delimit, from the left to the right, the cosmochemical, geochemical and geodynamical BSE models [17]. Best values from Borexino together with $\pm 1\sigma$ errors are reported: the experimental statistical and systematic uncertainties have been added in quadrature.

in the range 23–36 TW (see Fig. 4). The range of values includes the uncertainty on the distribution of heat producing elements inside the Earth. The model-independent analysis yields a radiogenic heat interval 11–52 TW (69% C.L.) for H(U + Th). Adopting the chondritic mass ratio above and a potassium-to-uranium mass ratio $m(\mathrm{K})/m(\mathrm{U}) = 10^4$, the total measured terrestrial radiogenic power is $\mathrm{P(U + Th + K)} = 33^{+28}_{-20}$ TW, to be compared with the global terrestrial power output $\mathrm{P_{tot}} = 47 \pm 2$ TW [14].

The contribution to the total geoneutrino signal from the local crust (LOC) is estimated to be $S_{\mathrm{geo}}(\mathrm{LOC}) = (9.7 \pm 1.3)$ TNU [15]. Considering the contribution from the rest of the crust (ROC) [16], the signal from the crust in Borexino is calculated as $S_{\mathrm{geo}}(\mathrm{LOC + ROC}) = (23.4 \pm 2.8)$ TNU. In order to estimate the significance of a positive signal from the mantle we have determined the likelihood of $S_{\mathrm{geo}}(\mathrm{Mantle}) = S_{\mathrm{geo}} - S_{\mathrm{geo}}(\mathrm{LOC + ROC})$ using the experimental likelihood profile of $S_{\mathrm{geo}}$ and a Gaussian approximation for the crust contribution. The nonphysical region, $S_{\mathrm{geo}}(\mathrm{Mantle}) < 0$, is excluded. This approach gives a signal from the mantle equal to $S_{\mathrm{geo}}(\mathrm{Mantle}) = 20.9^{+15.1}_{-10.3}$ TNU, with the null hypothesis rejected at 98% C.L.

An updated measurement of $\bar{\nu}_e$'s with Borexino is presented. We show that Borexino-only data measure geoneutrinos with $5.9\sigma$ significance. We also shows that the background level in Borexino allows us to perform a real time spectroscopy of geoneutrinos, currently limited only by the size of the detector.

## ACKNOWLEDGMENTS

The Borexino program is made possible by funding from INFN (Italy), NSF (USA), BMBF, DFG, and MPG (Germany), RFBR: Grants No. 14-22-03031 and No. 13-02-12140, RFBR-ASPERA-13-02-92440 (Russia), and NCN Poland (UMO-2012/06/M/ST2/00426). We acknowledge the financial support from the UnivEarthS Labex program of Sorbonne Paris Cité (ANR-10-LABX-0023 and ANR-11-IDEX-0005-02). We acknowledge the generous support and hospitality of the Laboratori Nazionali del Gran Sasso (LNGS). We acknowledge the collaboration of J. Mandula for providing detailed data on reactor load factors.

[1] G. Fiorentini, M. Lissia, and F. Mantovani, Phys. Rep. **453**, 117 (2007).
[2] G. Bellini, A. Ianni, L. Ludhova, F. Mantovani, and W. F. McDonough, Prog. Part. Nucl. Phys. **73**, 1 (2013).
[3] G. Bellini *et al.* (Borexino Collaboration), Phys. Lett. B **687**, 299 (2010).
[4] G. Bellini *et al.* (Borexino Collaboration), Phys. Lett. B **722**, 295 (2013).

[5] T. Araki *et al.* (KamLAND Collaboration), Nature (London) **436**, 499 (2005).
[6] S. Abe *et al.* (KamLAND Collaboration), Phys. Rev. Lett. **100**, 221803 (2008).
[7] G. Alimonti *et al.* (Borexino Collaboration), Nucl. Instrum. Methods Phys. Res., Sect. A **600**, 568 (2009).
[8] G. Alimonti *et al.* (Borexino Collaboration), J. Cosmol. Astropart. Phys. 08 (2013) 049.
[9] G. Bellini *et al.* (Borexino Collaboration), Phys. Rev. D **89**, 112007 (2014).
[10] E. Gatti and F. De Martini, Nucl. Electronics **2**, 265 (1962).
[11] A. Gando *et al.* (KamLAND Collaboration), Phys. Rev. D **88**, 033001 (2013).
[12] Nuclear Power Engineering Section, IAEA-PRIS database, http://www.iaea.org/pris/, Power Reactor Information System (IAEA-PRIS database).
[13] M. Baldoncini, I. Callegari, G. Fiorentini, F. Mantovani, B. Ricci, V. Strati, and G. Xhixha, Phys. Rev. D **91**, 065002 (2015).
[14] J. H. Davies and D. R. Davies, Solid Earth **1**, 5 (2010).
[15] M. Coltorti *et al.*, Earth Planet. Sci. Lett. **293**, 259 (2010).
[16] Y. Huang, V. Chubakov, F. Mantovani, R. L. Rudnick, and W. F. McDonough, Geochem., Geophys., Geosyst. **14**, 2003 (2013).
[17] O. Šrámek, W. F. McDonough, E. S. Kite, V. Lekić, S. T. Dye, and S. Zhong, Earth Planet. Sci. Lett. **361**, 356 (2013).